ASSOCIATED CONTENT

Supporting Information:

S1: XRD patterns of ZAS sonicated for different time period

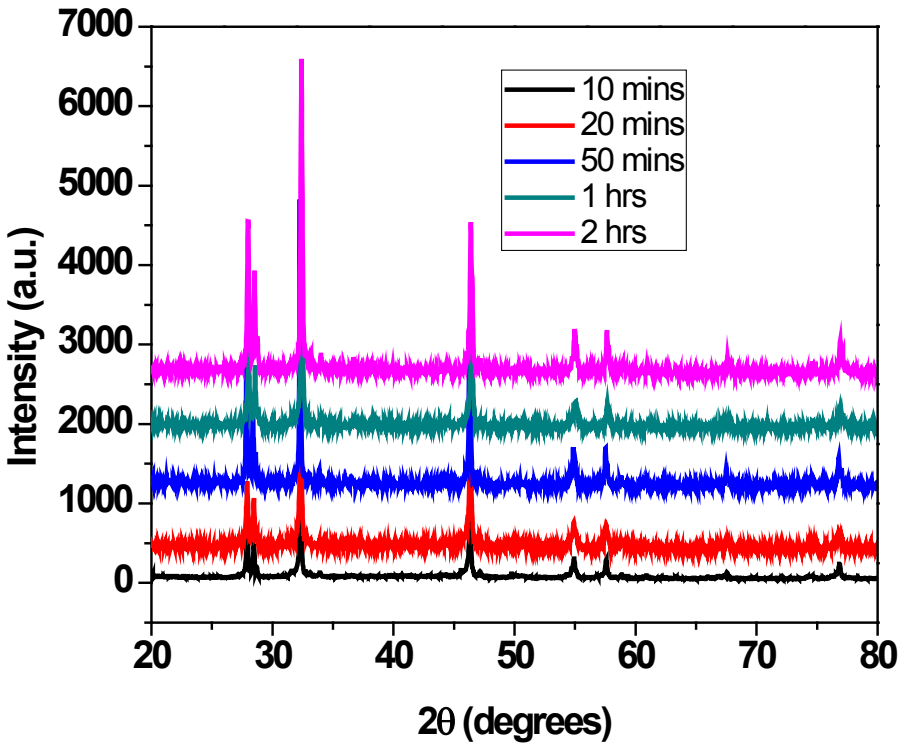

Figure S1 XRD patterns of ZAS sonicated for different time period

Fig.S1 shows the XRD patterns of ZAS compound sonicated for different time period. It can be clearly seen that single phase is confirmed in all the sonicated samples.

S2: XPS spectra of ZAS

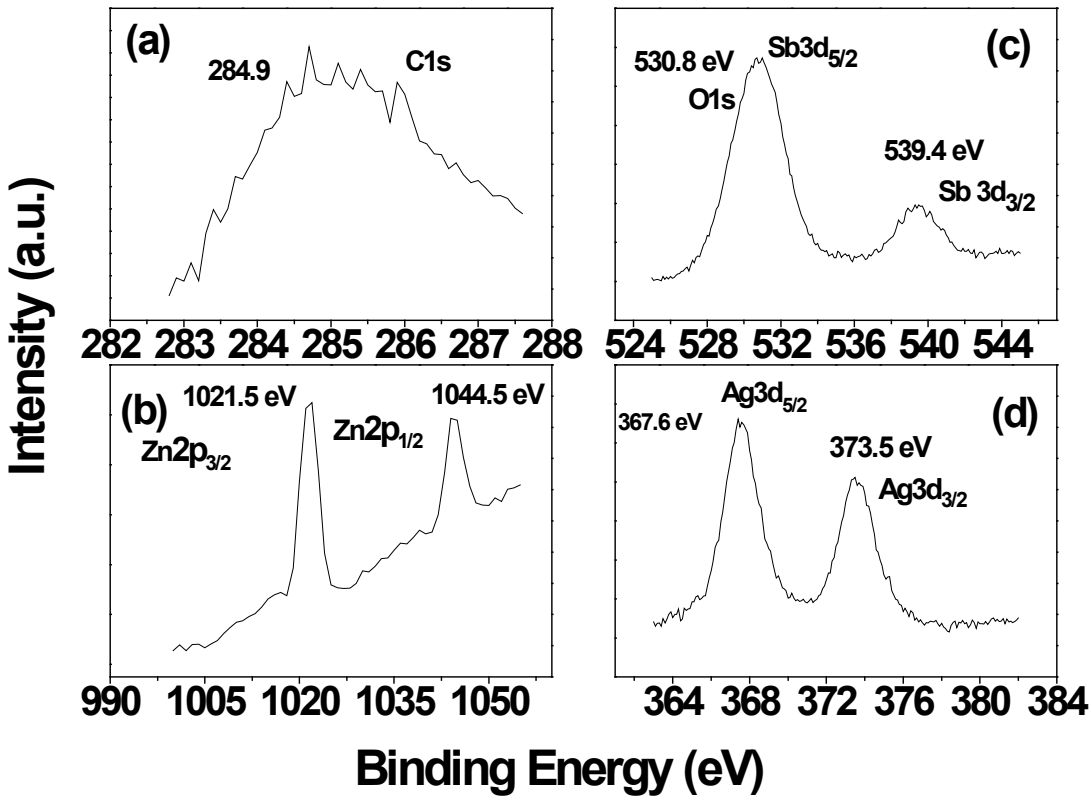

Figure S2 XPS spectra of ZAS

Fig.S2 shows the XPS spectrum of the nanostructured $ZnAg_3Sb_2O_4$ indicating the presence of Zn, Ag, Sb, O and C elements. The shift of binding energy due to relative surface charging has been corrected using the C 1s level at 284.9 eV as an internal standard. The XPS spectra of Zn are shown in Fig. S2(b). The appearance of peaks at 1021.5 eV and 1044.5 eV which corresponds to the $Zn2p_{3/2}$ and $Zn2p_{1/2}$ confirms the presence of Zn in the compound. Fig. S2 (c) shows the XPS spectrum of the Ag. There are two adjacent peaks observed at 367.6 eV and 373.5 eV corresponds to Ag $3d_{5/2}$ and Ag $3d_{3/2}$, respectively. Compared with the standard value of bulk Ag (368.2 eV), the $3d_{5/2}$ peak of Ag in our work shifts to lower binding energy. The XPS spectra of the O-1s and Sb 3d can be seen in Fig.S2 (d). Here $Sb3d_{5/2}$ peak overlaps with O1s peak. The distance between the $Sb3d_{5/2}$ and $Sb3d_{3/2}$ peak is observed to be ~ 8.6 eV and the peak area of Sb $3d_{5/2}$ is ~ 1.5 times that of $Sb3d_{3/2}$. The XPS also shows the ratio of the Zn: Ag: Sb: O (1.1:3.3:1:3.7) which is nearly agreement with the theoretical ratio (1:3:1:4).

S3 FTIR spectrum of ZAS

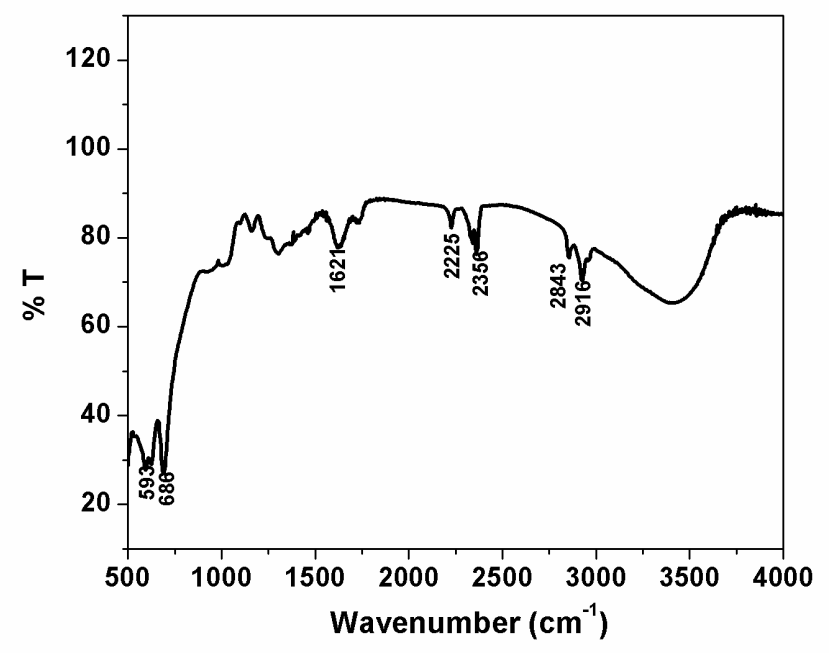

Figure S3 FTIR spectrum of ZAS

Fig. S3 shows the FTIR spectrum of ZAS. It can be seen that the band centered at 593cm^{-1} pertains to the characteristics of Zn-O stretching vibration band in a tetrahedral site. The strong peak of Ag-O band is observed at 686 cm$^{-1.}$ The appearances of relatively weak peaks at ~ 1300-1470 cm^{-1}, 1600cm^{-1} and 1700-2230cm^{-1} corresponds to the bending vibrations of C-H bond, C=O stretching and CO_2 bending mode, respectively. This may be due to the absorption of atmospheric CO_2. Generally, it is observed that in all transition based metal oxide materials which are prone to adsorption of CO_2.

S4XRD pattern of ZAS compound after the photocatalytic testing

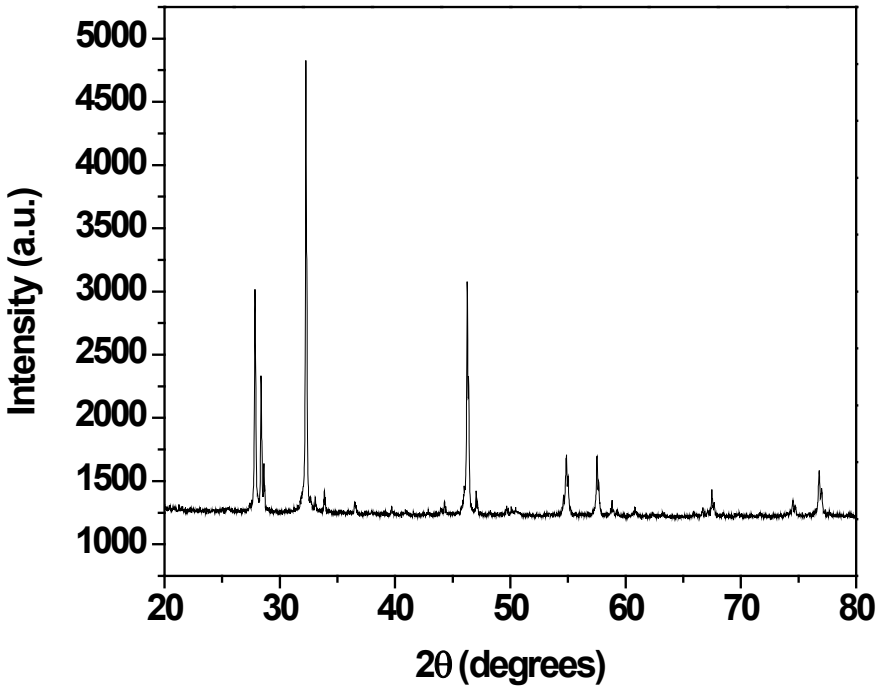

Figure S4 XRD pattern of ZAS compound after the photocatalytic testing

Fig. S4 shows the XRD pattern of the ZAS after the photocatalytic testing. No significant change was observed in the XRD pattern which confirms the stability of the ZAS photocatalyst. Figure S5 displays the UV-DRS pattern of ZAS compound after the photocatalytic testing. The UV spectrum was found to be almost similar to the UV spectra of the catalyst before hydrogen production.

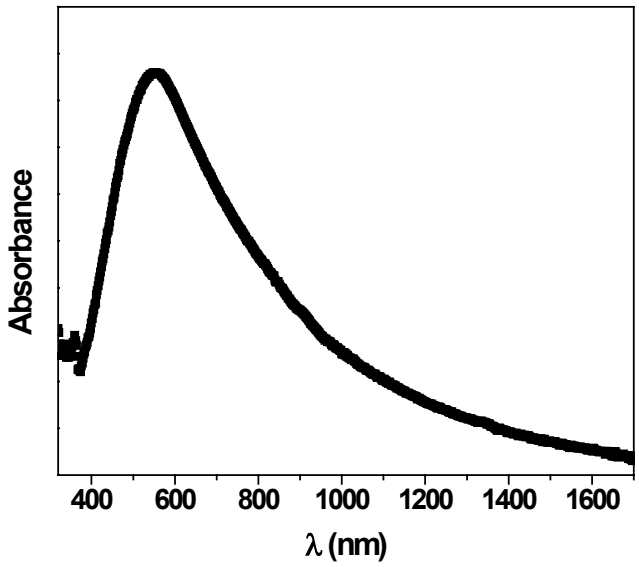

Figure S5 UV DRS Spectrum of ZAS compound after the photocatalytic testing

S6 Photocatalytic Testing:

A 300 W Xe lamp equipped with a cut-off filter at 420 nm was used to provide the incident visible light. The produced hydrogen gas was analyzed with gas chromatograph. The apparent quantum efficiency (AQE) was measured under the same reaction conditions and the lamp was equipped with a filter of wavelength 420 nm. The number of photons from the radiation source (1.16 x 10^{23} Photons/h) was measured using a silicon photodiode.

The following equation was used for the calculation of AQE.

$$AQE\ (\%) = \frac{Number\ of\ reacted\ electrons}{Number\ of\ incident\ photons} \times\ 100$$

$$= \frac{Number\ of\ H_2\ molecules\ evolved\ \times\ 2}{Number\ of\ incident\ photons} \times\ 100$$

$$= \frac{2 \times 6.14 \times 10^{21}}{1.16 \times 10^{23}} \times 100$$

$$= 10.6$$

S.7 Effect of KOH concentration on the H_2 Production:

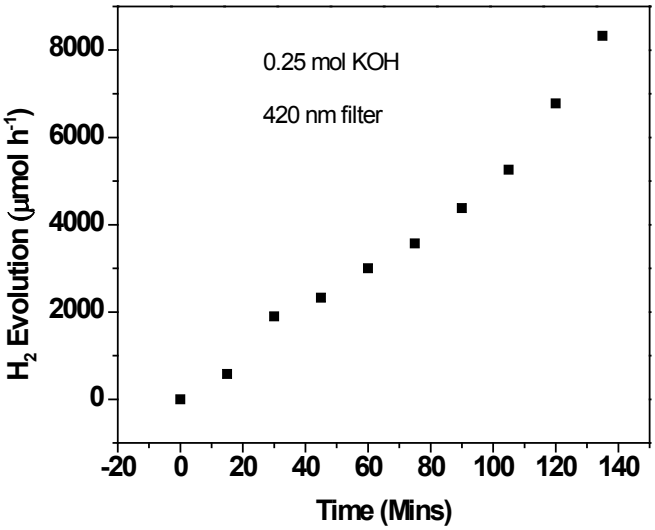

Fig. S6 Photocatalytic performance of ZAS for hydrogen generation at 0.25 mol KOH solution

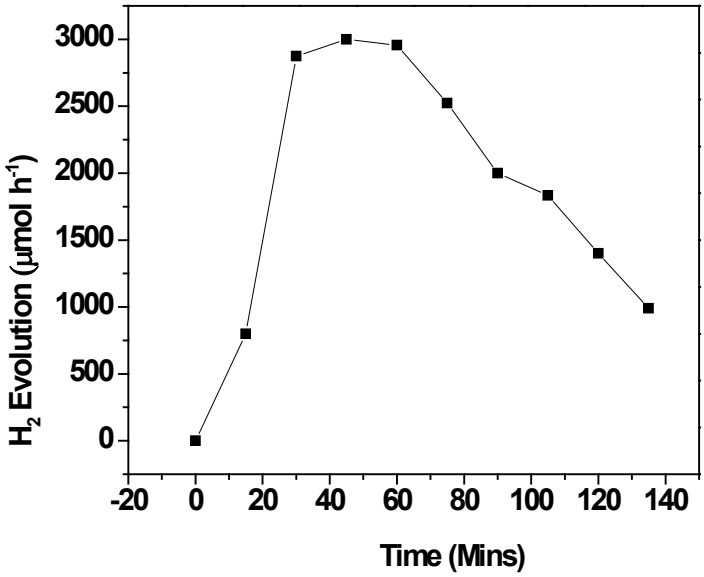

Fig. S7 Photocatalytic performance of ZAS for hydrogen generation at 0.75 mol KOH solution

Initially, in order to optimize the rate of hydrogen production, we have measured the H_2 production with different concentration of KOH content. It was observed that at lower as well as at higher KOH content, the amount of H_2 produced was decreased. This may be due to the fact

that at higher KOH conc., initially with increase in reaction time increment in H_2 generation was observed but with further increase in reaction time decrement in the production rate was observed which can be ascribed to the degradation of the catalyst due to excess KOH. Whereas, in case of lower KOH content the amount of H_2 produced was lower than the 0.5 mol KOH which is because of the lower dissolution of H_2S. Hence, the optimum concentration of KOH is 0.5 mol. which was applicable to almost all catalysts. This study has been performed several time. Hence, all photoreactions were performed at this optimized KOH concentration i.e. 0.5M. Therefore, in the manuscript we have only presented the optimized data.

S8: Preliminary trails on Dye (MB) degradation

The preliminary trials of MB (20 ppm) degradation were conducted under natural sun using 0.5gm ZAS. There is almost complete degradation under sun light on sunny days within two hrs. However, we need to optimize the catalyst for different concentration under natural sunlight. The further work is in progress.

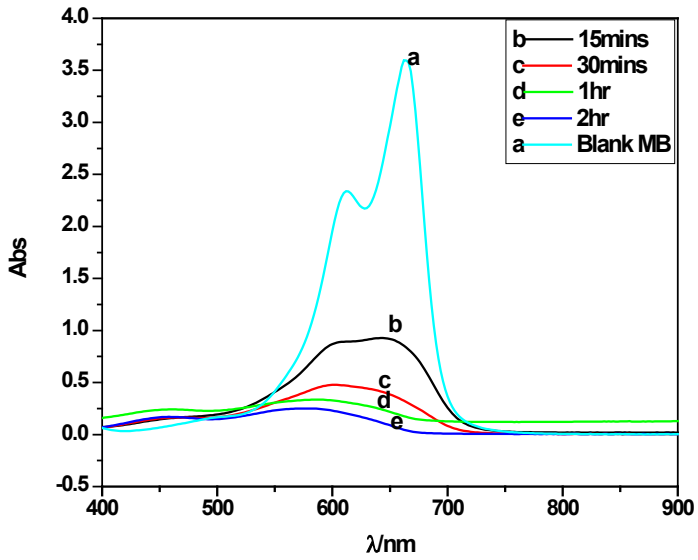

Fig. S 8: UV-visible spectra of degraded samples